

# Optical Pumping

Shreya Nagpal  
Lab Partner: Susanna Weber  
October 20, 2022

## Abstract

This lab concerns the technique of optical pumping as a method to measure the energy level differences of the ground states of atoms. Specifically, optical pumping is performed on two Rubidium isotopes in this lab in order to examine the structure of their ground states. This setup can be used to measure other properties of nature as well, including the spins of the two isotopes and the ambient magnetic field of the apparatus used. Our results agree with known values, signifying that this instrumentation and procedure can accurately probe the structure of atoms and can also serve as a magnetometer for small magnetic fields.

## 1 Introduction

Through a technique called optical pumping, this experiment aims to observe the frequencies at which transitions occur between Zeeman energy levels on two different Rubidium isotopes. Optical pumping allows the close measurement of Zeeman splitting energy levels of atoms in the presence of a magnetic field [Zaf60]. In this experiment specifically, it is conducted on gaseous Rubidium-85 and -87 isotopes inside a bulb.

When a sample of gaseous Rubidium atoms is placed in a static magnetic field, the atoms undergo fine-structure, hyperfine, and Zeeman splitting. Optical pumping is a technique by which polarized light is used to “pump” these atoms to the highest possible ground state energy level. With the gas no longer capable of absorbing energy, light can then be observed passing through the gas.

Optical pumping is conducted on a spin-polarized gas. This technique is carried out by exciting atoms from the  $S_{1/2}$  to  $P_{1/2}$  state using circularly-polarized light. Due to spontaneous emission, half of these states will return to the ground state; the other half will fall to the  $m_F = 1$  state, following selection rules. When the atom falls from the excited state to the ground state, the magnetic quantum number is changed by either 1 or 0 and a photon is emitted. If the atoms at the ground  $S_{1/2}$  state are continually excited, including the fraction of atoms that fall back to the ground state after excitation, then the gas will approach a state where all Rb atoms are at the  $m_F = 1$  state – this is what it means for atoms to be “pumped.”

Once a gas is pumped and the magnetic field is no longer affecting it, a radiofrequency (RF) field can be applied, causing atoms to leave the pumped state and begin absorbing light again. By measuring the light that passes through the Rubidium gas as well as the frequency of the RF signal at different currents, the resonant Zeeman frequency and nuclear spins of the two isotopes can be found. We can also use this information to measure the local magnetic field strength of the Earth.

## 2 Theory

### 2.1 Zeeman Splitting

Using the degenerate theory of quantum mechanics, we can find the fine and hyperfine corrections to the energy levels of atoms. With the additional application of the magnetic field, the Rubidium atoms undergo Zeeman splitting [Lab]. We can use perturbation theory to calculate the resonant Zeeman frequency:

$$E = H\nu = g_F\mu_B B \quad (1)$$

where

$$g_F = g_J \frac{F(F+1) + J(J+1) - I(I+1)}{2F(F+1)},$$
$$g_J = 1 + \frac{J(J+1) + S(S+1) - L(L+1)}{2J(J+1)}$$

Here,  $g$  is the Lande factor and  $J$  and  $F$  are the fine and hyperfine energy levels. More specifically:  $J$  is the net orbital angular momentum,  $I$  is the nuclear spin, and  $F = J + I$  is the total angular momentum of the atom. Zeeman splitting additionally involves  $m_F$ , which is the magnetic quantum number that labels the Zeeman energy levels [Oue10]. The Zeeman transitions we are considering increase  $m_F$  by 1.

Figure 1 shows the energy levels of a Rubidium atom. In this lab, we are interested in measuring the transitions between Zeeman levels  $m_F$ .

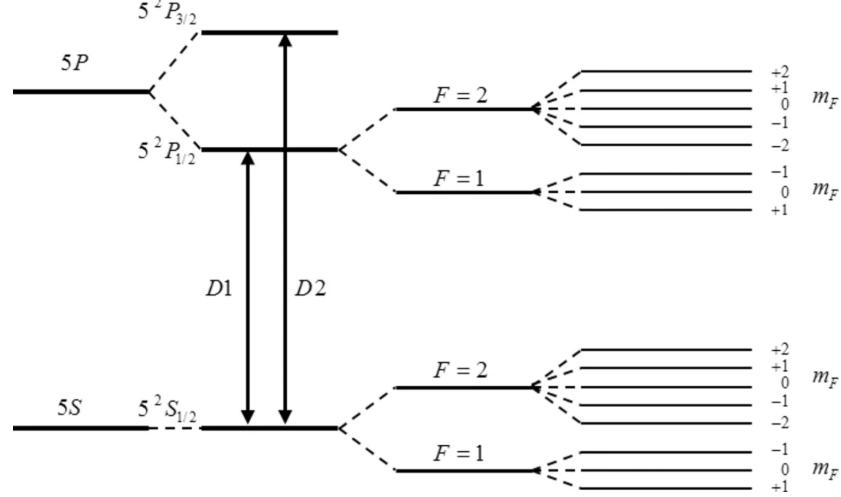


Figure 1: Fine, hyperfine, and Zeeman splitting in a Rubidium atom [Lab]

## 2.2 Calculating the Resonant Zeeman Frequency

Now, using  $J = \frac{1}{2}$ ,  $S = \frac{1}{2}$ ,  $L = 0$ , and  $F = 0$ , we can derive the *Breit-Rabi equation*:

$$\frac{\nu}{B_{ext}} = \frac{2.799}{2I + 1} \quad (2)$$

where  $\nu$  is the Zeeman resonant frequency,  $B_{ext}$  is the external magnetic field, and  $I$  is the nuclear spin. This formula, along with Equation 1, can be used to calculate the ground state Zeeman energies.

The magnetic field  $B_{ext}$  is applied by the Helmholtz coil in this experiment, the magnitude of which can be determined with

$$B_H = 0.9 * 10^{-2} \frac{Ni}{a} \frac{Gm}{A} [\text{Lab}], \quad (3)$$

where  $N$  is the number of turns in the coil,  $a$  is the radius of the coils, and  $i$  is the current flowing through them. Equations 2 and 3 together mean that we can derive the resonant Zeeman frequency given the current.

## 3 Methods

### 3.1 Apparatus

The bulb of rubidium gas is placed inside a metal box with the heating and polarizing equipment as well as the photodetectors to avoid noise from ambient light. This equipment consists of a lamp to pump Rubidium atoms from the ground state as well as a circular polarizer and band pass filter that work in tandem to ensure that  $\Delta m_F = 0$  or 1. The metal box is placed between two Helmholtz coils, which receive signal through a function generator and generate a magnetic field.

This polarized, filtered light inside the metal box enters the glass bulb containing the Rubidium gas, which is comprised of the Rubidium-85 and Rubidium-87 isotopes (where  $I = \frac{5}{2}$  and  $\frac{3}{2}$  respectively) [Zaf60]. This bulb additionally contains a photodiode, the light of which can appear dimmer or

brighter to the photodetectors depending on the state of the gas surrounding it. The signal from the photodetectors is amplified and then fed into an oscilloscope.

The current signal sent to the Helmholtz coils has two components: AC and DC. The AC component is sent by the oscilloscope and allows us to view the scope output to determine resonance. The DC component of the current signal is sent from a power supply and is varied throughout the experiment to explore various Zeeman resonance frequencies. The DC component of the current signal can be measured using the voltage drop across a shunt resistor.

Finally, this entire setup is tilted to align with the direction of Earth’s magnetic field, ensuring that the magnetic field vectors only add. Figure 2 is a picture of the full setup and Figure 3 offers a detailed block diagram of the setup.

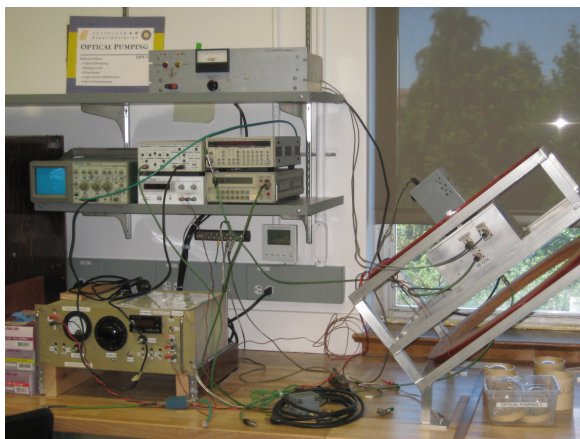


Figure 2: Full experimental setup [Lab].

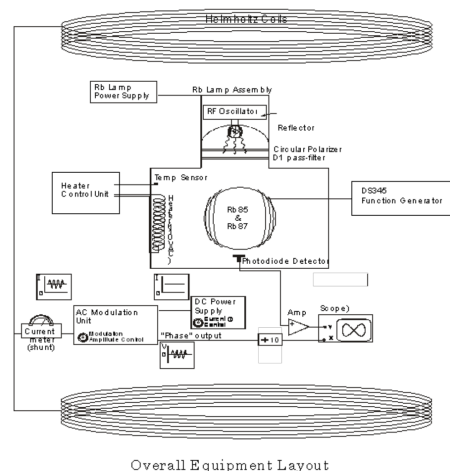


Figure 3: Block diagram of the setup [Lab].

### 3.2 Procedure

There are two ways in which the Zeeman resonance frequency is determined: ODMR and lock-in detection.

### 3.3 First Approach: ODMR

The first approach is called “optically detected magnetic resonance,” or ODMR, in which the results collected by the photodetector indicate resonance. The idea is as follows: if the atoms are driven by a resonant RF field, then the atoms will all be driven out of the optically pumped state, allowing them to absorb light and yielding low light level readings on the photodetector. The opposite is true for a non-resonant RF field, with the atoms being unable to absorb additional light and the photodetector readings being high.

The following steps are followed to detect and measure Zeeman resonance with this technique:

1. Turn on the DC current, creating a magnetic field in the Helmholtz coils and inducing Zeeman splitting in the Rubidium atoms.
2. Turn on the circularly-polarized light, creating a spin-polarized Rubidium gas.
3. Turn on the heater to optically pump the Rubidium.
4. Send a sinusoidal current with a linear sweep of frequencies through the function generator into the Helmholtz coils.
5. Set the oscilloscope to X-Y mode to see the photodiode signal vs. the field frequency.

After carrying out this procedure, we can observe two peaks on the oscilloscope, one corresponding to each isotope (see Figure 4 for an example).

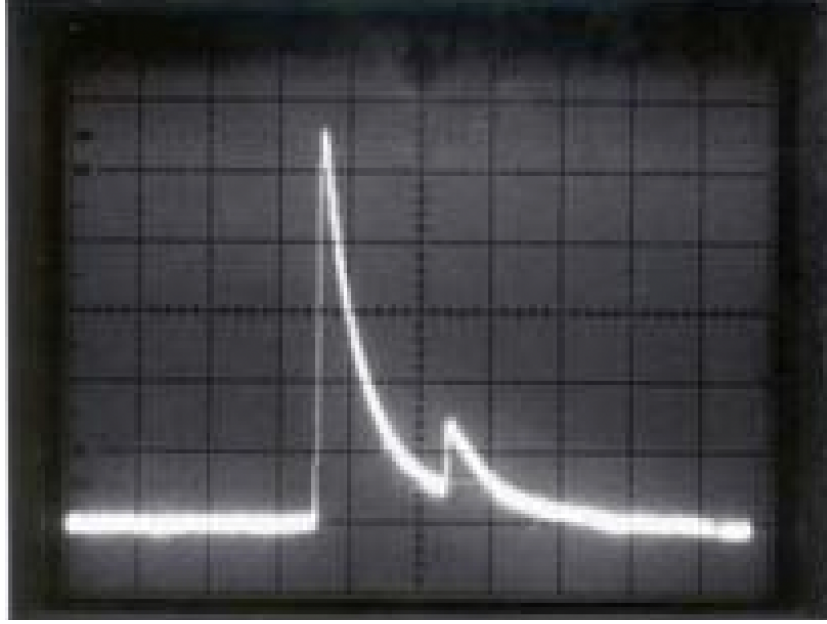


Figure 4: Sample ODMR output. The larger peak correlates with the more common isotope. [Lab]

### 3.4 Second Approach: Lock-in Detection

The second approach to detecting Zeeman resonance is lock-in detection, which involves sweeping through various values of the Helmholtz current while keeping the magnetic field at a constant frequency.

The following steps are followed to detect and measure Zeeman resonance with this technique:

1. Prepare an optically pumped gas as described previously.
2. Switch on the field modulation, sending a 60 Hz constant frequency into the Helmholtz coils and then measuring the variation of the measured signal at the modulation frequency.
3. Plot signal variation vs. photodiode voltage on the oscilloscope, searching for a symmetric *Lissajous curve*.

The curve plotted is called a Lissajous curve, which serves as an indicator for resonance. If this curve is symmetrical, then it signals Zeeman resonance. Figure 5 is an example of a Lissajous curve indicating resonance.

Since much of this technique relies on visual confirmation of symmetric Lissajous curves, it is important to measure several different forward and reverse current values and take multiple measurements at each point to be confident in our results. As we performed this experiment, for example, we took four separate measurements of the frequency at which we observed symmetry and did so for seven different current values. Each current value has resonance at two different frequencies, one for each isotope.

## 4 Results and Analysis

### 4.1 Current vs. Resonance Frequency Plots

The following figures are the resultant data points of resonance frequency measurements at various DC current values for lock-in detection. The fit is a weighted fit using linear regression as described in reference [Lyo91], yielding slope, intercept, and  $\chi^2$  values of:

- $m = 2.03 \pm 0.002 \text{ MHz/A}$ ,  $b = 0.18 \pm 0.003 \text{ MHz}$ ,  $\chi^2 = 18.32$  for Rb85 forward current
- $m = -1.94 \pm 0.003 \text{ MHz/A}$ ,  $b = 0.085 \pm 0.006 \text{ MHz}$ ,  $\chi^2 = 17.55$  for Rb85 reversed current

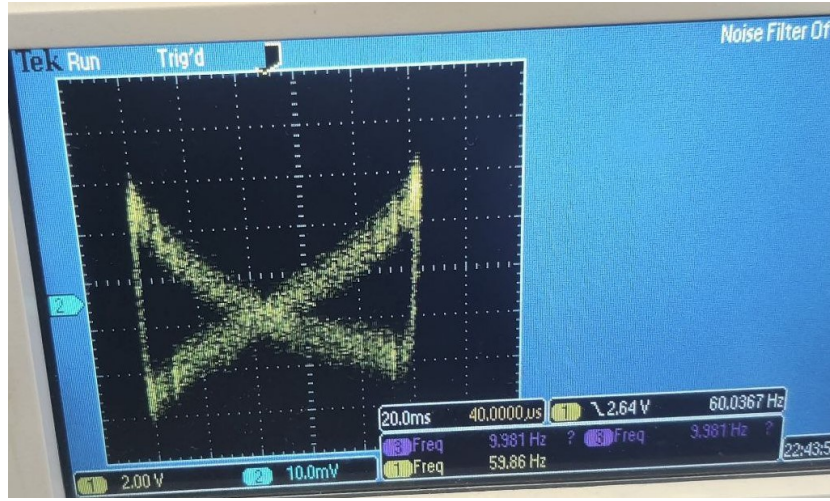


Figure 5: A Lissajous curve at resonance.

- $m = 3.01 \pm 0.002 \text{ MHz/A}$ ,  $b = 0.29 \pm 0.004 \text{ MHz}$ ,  $\chi^2 = 607.4$  for Rb87 forward current
- $m = -2.92 \pm 0.004 \text{ MHz/A}$ ,  $b = 0.097 \pm 0.008 \text{ MHz}$ ,  $\chi^2 = 928.41$  for Rb87 reversed current.

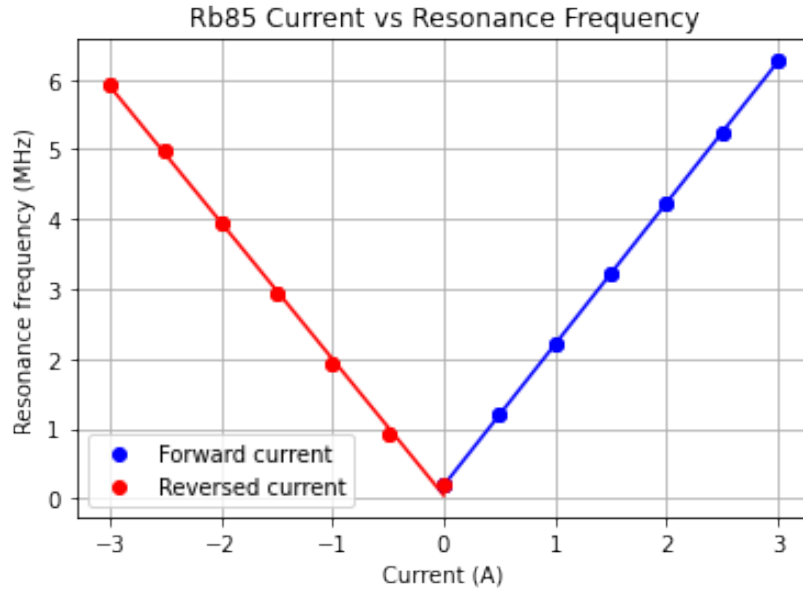


Figure 6: Current vs frequency for Rubidium-85 (weighted)

The weights of each point are calculated using the standard error  $\frac{\sqrt{\sigma}}{N}$  (where  $N = 4$  for 4 data points per current). These errors are included on the graph as error bars, though they are too small to be seen on the MHz scale of the plots.

The  $\chi^2$  values are generally very large, which indicates an appropriate fit with data that is unrealistically precise. This is likely due to our use of a digital oscilloscope for while examining Lissajous curves. The digital oscilloscope was low-resolution and caused our observation of the range of frequency values to be inaccurately small. This resulted in a small standard deviation, which then results in a very large  $\chi^2$ .

Unweighted fits are also performed on the data, with the sum squared of residuals as errors here:

- $m = 2.03 \pm 0.003 \text{ MHz/A}$ ,  $b = 0.18 \pm 0.01 \text{ MHz}$ ,  $\chi^2 = 47.51$  for Rb85 forward current

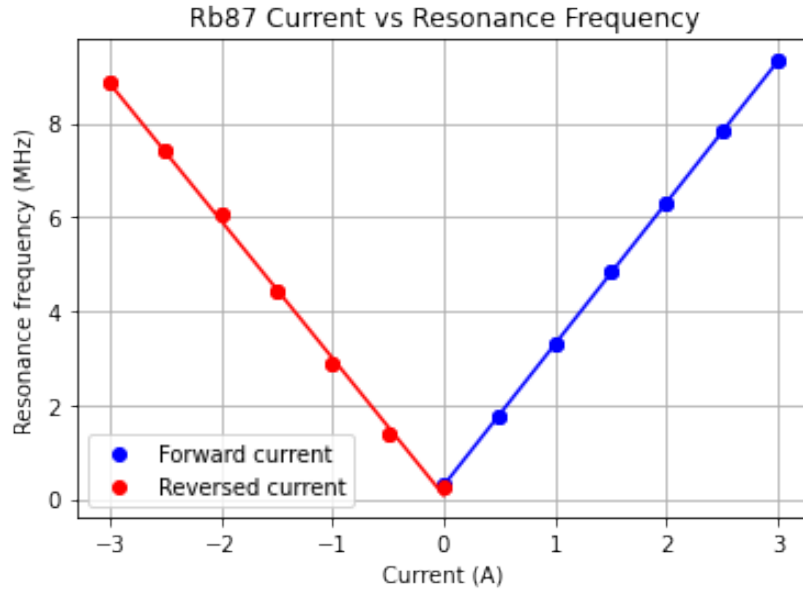


Figure 7: Current vs frequency for Rubidium-87 (weighted)

- $m = -1.96 \pm 0.003 \text{ MHz/A}$ ,  $b = 0.042 \pm 0.06 \text{ MHz}$ ,  $\chi^2 = 18.13$  for Rb85 reversed current
- $m = 3.01 \pm 0.002 \text{ MHz/A}$ ,  $b = 0.29 \pm 0.009 \text{ MHz}$ ,  $\chi^2 = 671.27$  for Rb87 forward current
- $m = -2.92 \pm 0.04 \text{ MHz/A}$ ,  $b = 0.083 \pm 0.1 \text{ MHz}$ ,  $\chi^2 = 1748.29$  for Rb87 reversed current.

These unweighted fits agree with the weighted fits and provide evidence that the fits are generally good despite the high  $\chi^2$  values.

One final graph consists of the reverse-current values being negated and fitted (via weighted linear regression as before) to the same line as the forward-current values for each isotope:

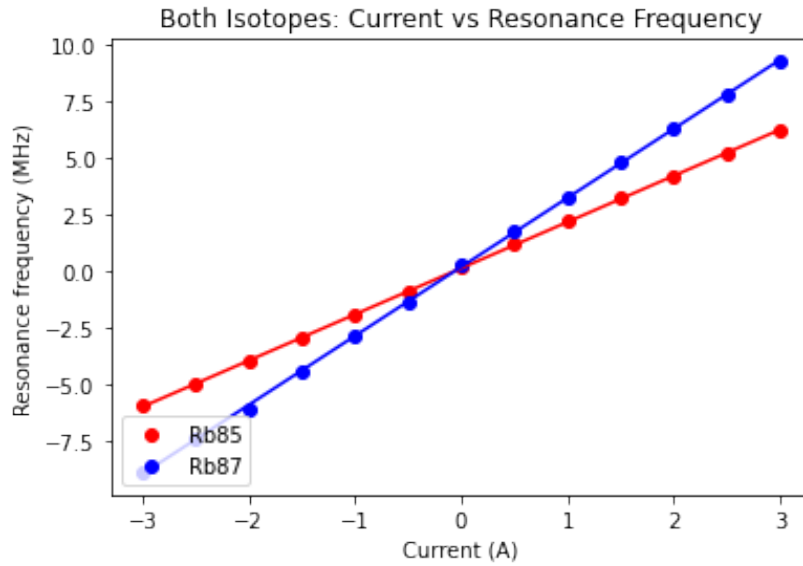


Figure 8: Current vs frequency for both isotopes

For the combined fit, we find:

- $m = 2.042 \pm 0.004 \text{ MHz/A}$ ,  $b = 0.145 \pm 0.01 \text{ MHz}$ ,  $\chi^2 = 412.00$  for Rb85.



- $m = 3.053 \pm 0.01 \text{ MHz/A}$ ,  $b = 0.203 \pm 0.020 \text{ MHz}$ ,  $\chi^2 = 1095.70$  for Rb87.

With error bars generated similarly to before, they are once again too small to be visible on this plot. Consequently, our  $\chi^2$  values are very large again, despite a fit that is quite good based on inspection.

## 4.2 Nuclear Moments of Isotopes

There are two ways to calculate the nuclear moments of these isotopes with the data collected. The first method is by finding the ratio of the nuclear moments and using it to calculate the respective nuclear moments.

An expected value for this ratio can be found by referring back to equation 2 and plugging in known values for  $I$  ( $3/2$  and  $5/2$ ) to find  $\frac{\nu_{87}}{\nu_{85}} = \frac{3}{2}$

To find experimental results, we must first create a graph of Rb85 resonance frequencies vs Rb87 resonance frequencies (see Figure 9) and find the slope of the line of best fit.

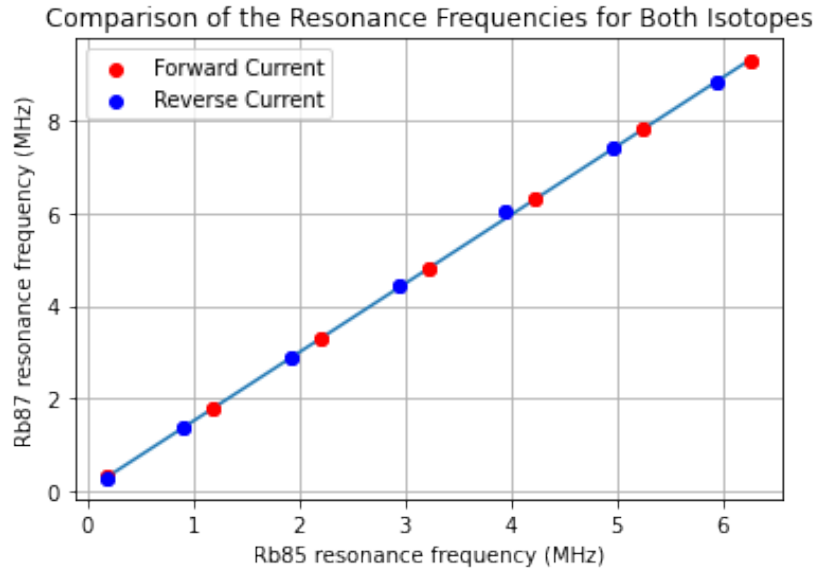


Figure 9: Rb85 Resonance Frequencies vs Rb87 Resonance Frequencies

The slope and intercept, via linear regression again, are  $1.486 \pm 0.02$  and  $0.02 \pm 0.008$  (approximately 0) respectively. This value agrees with the predicted value of 1.5.

Now, to calculate the nuclear moment for each isotope, we can plug in the calculated ratio back into the Breit-Rabi equation 2 and find

$$\frac{\nu}{i} = \frac{2.799}{2I + 1} \frac{0.9 \times 10^{-2} N}{a}$$

where  $N = 137$  loops,  $a = 27.5\text{cm}$  (radius of coils), and the ambient field of Earth is treated as negligible. Upon solving for the individual nuclear moments, we find that it is  $2.57 \pm 0.145$  for Rb85 and  $1.55 \pm 0.205$  for Rb87. These results agree with the known values of 2.5 and 1.5, indicating that the data is valid and the approximation of ignoring the local magnetic field is reasonable.

## 4.3 Estimate of Local Magnetic Field Strength

In reality, ignoring the local magnetic field of the Earth in the previous section is just an approximation. This setup can be used to estimate this field with two methods, the results of which can be compared for agreement.

The first method is to turn off the current to the Helmholtz coils entirely and then measure the frequency at which resonance can be observed.  $B_{ext}$  can be calculated using this frequency and equation

2. Resonance was recorded for both isotopes, with corresponding field strengths of  $0.41 \pm 0.01$  G for Rb85 and  $0.42 \pm 0.01$  G for Rb87.

The second approach is to use the y-intercepts from the current vs. frequency graphs as the frequency in the Breit-Rabi formula 2 to calculate B. This yields the field strength needed to *cancel* the ambient field, so reversing the direction of this calculated field reveals the estimate for Earth's magnetic field. Using this method, the estimates are  $0.41 \pm 0.02$  G for Rb85 and  $0.43 \pm 0.03$  for Rb87.

These estimates all agree with each other, but they do not agree with the known magnetic field strength in Berkeley, which is 0.48 G [NOA]. This difference may be due to other local magnetic fields in the room such as electronic devices.

#### 4.4 Observed Resonance in the Absence of a Magnetic Field

Upon cancelling out the measured ambient field by inducing a negative magnetic field in the Helmholtz coil of the same magnitude, resonance can still be observed. This resonance is at a current of 0.9 A, which creates a magnetic field of  $.39 \pm 0.046$  G. Though an odd occurrence at first, this small magnetic field can be explained by edge effects – there are still locations further from the center of the coils where the field is not correctly cancelled. Modulations called Rabi oscillations (Figure 10) can be observed in the photodiode signal. Rabi oscillations occur in superpositioned two-state systems that evolve over time – here, the system is in a superposition of being pumped and relaxed.

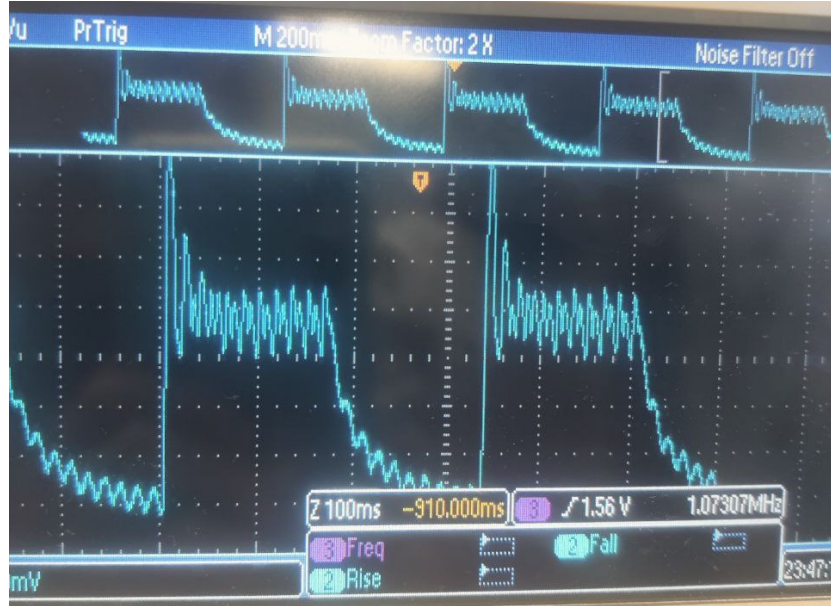


Figure 10: Rabi oscillations visible with square wave input modulation of a sinusoidal signal.

#### 4.5 Analysis of Time Scales

To find the pumping and relaxation times, the Helmholtz coils can be driven by a square wave amplitude modulated sinusoidal signal at a resonance frequency from the function generator. This photodiode signal is shown in Figure 10. In this output, repeated optical pumping and relaxation is evident, along with the aforementioned Rabi oscillations.

The relaxation time can be determined by inspection of this output to be approximately  $1.510^{-6}210^{-6}$  and the pumping time is approximately  $110^{-7}210^{-7}$ . These are the average of four separate measurements, between which the oscilloscope was turned off and back on. The errors on these measurements are simply the standard error of the four measurements. The theoretical value to compare this to, though out of scope for this particular report, can be found using Fermi's Golden Rule [Fou22]. This rule describes a system in which an eigenstate of a Hamiltonian is perturbed. A decay probability can be calculated through this approach, which is related to the mean lifetime and thus the pumping



and relaxation rates [Fou22]. Though doable, this calculation would require a detailed understanding of quantum mechanics that is currently outside the scope of this report (but would make a very interesting extension to this analysis!).

## 5 Conclusion

By conducting optical pumping on a spin-polarized Rubidium gas and then driving the atoms with an RF-induced magnetic field, we were able to observe Zeeman splitting and measure the resonance frequencies of Zeeman splitting in Rubidium atoms. Careful analysis of the data yielded experimental values for the nuclear moments of the two Rubidium isotopes, an estimate of local magnetic field strength, and time scales of pumping and relaxation. We were also able to qualitatively identify Rabi oscillations. We calculated theoretical values to compare our experimental findings with and commented on agreement.

## References

- [Fou22] Wikimedia Foundation. Fermi's golden rule. *Wikipedia*, 2022.
- [Lab] Physics 111B: Advanced Experimentation Laboratory. Opt - optical pumping.
- [Lyo91] L. Lyons. A practical guide to data analysis for physical science students. *Cambridge University Press*, 1991.
- [NOA] NOAA. Magnetic field calculators. *National Oceanic and Atmospheric Administration*.
- [Oue10] Jonathan Ouellet. Energy level diagrams for rb. 2010.
- [Zaf60] R.L. De Zafra. Optical pumping. *American Journal of Physics* 28, 646, 1960.